

MULTI-RESPONSE OPTIMIZATION IN AA6063/SS304 BIMETALIC FRICTION WELDING USING TAGUCHI GREY RELATIONAL ANALYSIS

S. Senthil Murugan^{1,2*}, M. Vishnoi^{3*},
S. Kattimani², T. G. Mamatha⁴

¹Department of Mechanical Engineering, Rajalakshmi Engineering College (Autonomous), Chennai, Tamilnadu, India

²Department of Mechanical Engineering, National Institute of Technology Karnataka, Surathkal, Karnataka, India

³Department of Mechanical Engineering, JSS Academy of Technical Education Noida, Uttar Pradesh, India

⁴Department of Mechanical Engineering, JSS University, Noida, 201301, Uttar Pradesh, India

*Corresponding authors' email address: vishnoi.mohit06@gmail.com, gctsegan@gmail.com

ABSTRACT

This study aimed to create a robust joint between dissimilar materials, specifically AA6063-T6 aluminium alloy and SS304 austenitic stainless steel (ASS), and optimize the parameters. The experiments were conducted by employing the rotary friction welding (RFW) process, with an experimental setup devised on a conventional lathe machine utilizing friction-generated heat and plastic deformation. The joint's performance was evaluated as per ASTM standards through hardness and Charpy impact tests, demonstrating favourable results and the results were used for further analysis. Higher hardness was observed at higher friction pressure with higher speed of rotation. It reached a maximum of 85 HRC. Conversely, the maximum impact energy was obtained at low speed with 32 J. According to microstructure of the dissimilar joint, very narrow welding interface (WI) was found, which is less than 20 microns in width. The Taguchi-Grey relational analysis (GRA)-L9 method with Minitab software was utilized for optimize the process parameters, providing insights into effective parameter selection and multi-response optimization for improved performance. The results indicated that the welding speed was the most influential parameter. Weld pressure also influenced the weld zone's hardness. Through the results, it is confirmed that RFW is emerged as a promising method for creating dissimilar joints, surpassing the limitations of fusion welding techniques.

KEYWORDS: Friction welding, dissimilar joint, Taguchi method, impact energy, Minitab software

1. INTRODUCTION


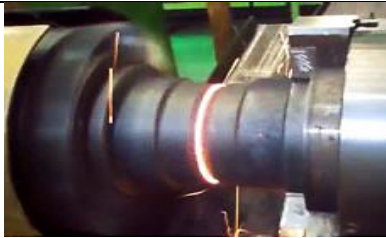

In various mechanical applications, components often necessitate a blend of diverse properties within a single unit, prompting the demand for joining dissimilar metals. This practice unlocks the potential to harness the distinctive advantages of different materials, offering tailored solutions to engineering challenges. The motivation behind dissimilar metal joining lies in amalgamating the superior mechanical properties of one material with the lightweight nature, corrosion resistance, or electrical conductivity of another. As a result, joining techniques for dissimilar materials have garnered significant interest in recent times [1]. Notably, there exists a considerable contrast in melting temperatures between aluminium (approximately 660°C) and steel (approximately 1538°C). This


divergence implies that aluminium tends to melt and flow away long before steel reaches its melting point. Among the various methods explored, friction welding stands out as the most effective approach for welding aluminium and stainless steel. Friction welding has firmly established itself as a solid-state welding process, finding application across a spectrum of industries including aerospace, automotive, defence, and beyond. Friction welding stands as a solid-state process devoid of electric or other external power sources, leveraging mechanical energy generated by friction at the interface of the components to be welded. Throughout the welding procedure, the surfaces are subjected to pressure, constituting the heating phase, which persists until the temperature required for plastic deformation is attained. Within the friction welding process, the components slated for joining are rotated against each other while a certain axial force (friction

force) is applied. This rotational movement serves to disrupt surface oxide layers, generating heat at the weld interface through friction, thereby locally softening the materials. As rotation continues, heat generation escalates, prompting plastic deformation of the materials at the weld interface. Concurrently, the fractured oxide layers are displaced from the weld interface via outward plastic metal flow, often observable as a flash, facilitating intimate contact between metal surfaces. Subsequently, the components are abruptly halted, and a higher axial force is exerted to finalize the weld [2]. This application of axial force ensures close contact between the components and induces plastic deformation of the material near the weld interface [3]. The strength of the joints exhibits variation with increasing upset pressure and upset time while maintaining constant friction pressure and friction time. Joint strength displays an initial increase followed by a gradual decrease after reaching peak values as upset pressure and upset time are elevated [4]. Certain welds exhibited diminished strength attributed to the buildup of alloying elements at the joint interface [5]. Despite widespread use, fusion welding processes continue to encounter numerous challenges in material joining. These include, firstly, the high viscosity of the molten welding pool in composite materials, impeding smooth flow and hindering effective mixing with filler materials. Consequently, the welding process struggles to achieve satisfactory weld formation and joint quality [6]. RFW emerges as a formidable method for achieving joints between dissimilar materials, a feat often unattainable through fusion welding processes. Metals and alloys that defy fusion welding methods

find compatibility with friction welding. The friction generated between surfaces facilitates a swift temperature elevation at the bonding interface, inducing plastic deformation of the material mass. This deformation, influenced by applied pressure and centrifugal force, results in material flow and the formation of a flash [7]. Notably, in RFW, cylindrical parts are imperative for successful execution [8]. Within welding processes, crucial parameters include RPM, surface forging force, flywheel mass, and forging time [9]. The strength of joints undergoes variation with increasing friction time, spindle speed, and the utilization of distinct pressure values [10]. The present investigation employed a continuous drive friction welding machine, a system characterized by rotating one workpiece at a consistent speed while aligning it with the second part under applied pressure. This rotational and pressure application persists for a specific duration to ensure optimal thermal and mechanical conditioning of the interface region. Subsequently, rotation ceases, often facilitated by forced braking, while simultaneously increasing pressure to forge the parts together. The primary objective of this study is to facilitate the joining and evaluation of solid-state joints between dissimilar materials, specifically AA6063 aluminium alloy and AISI 304 stainless steel while determining the optimal pressure for achieving a weld between aluminium and steel. Table 1 illustrates the sequential stages [11] of friction welding during the welding process, encompassing three main phases to weld the metals. Figure 1 depicts the relationship of welding parameters over a while.

Table 1. Stages of RFW

Steps	Explanation	Visual
1	Contact and rotate: One component is secured in a stationary clamp, while the second part is placed within the rotating spindle, which is subsequently brought up to a predetermined rotational speed. When the timing is right, a predetermined axial force is applied.	
2	Friction weld: In the subsequent step, friction pressure is exerted until the desired temperatures and material conditions are achieved. This phase facilitates the plasticization of both materials, and these conditions are upheld for a specified duration.	
3	Upset applied: The rotational speed is halted, followed by the application of increased axial force to generate "forge pressure" for a predetermined duration, thereby finalizing the weld. This process fosters molecular bonding and grain refinement across the weld zone.	

Steps	Explanation	Visual
4	Complete: The finish friction weld was ready after upsetting and quenching for further flash removal.	

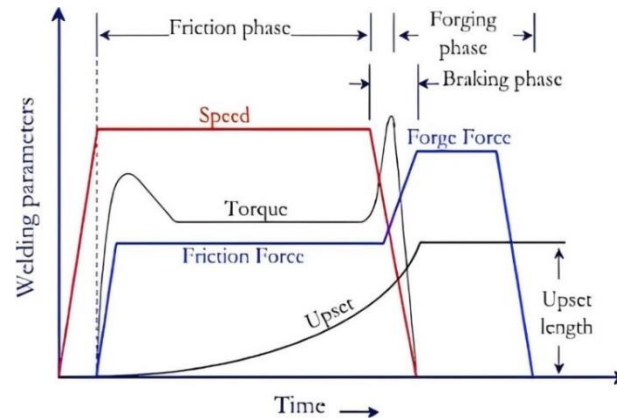


Fig. 1. Friction welding parameters vs. time [12]

2. MATERIALS AND METHODS

2.1. Materials

This study employed AA6063-T6 and AISI304 alloys for the friction welding work. AA6063 is the

nonferrous aluminium category and AISI304 is the austenitic stainless steel, which is familiar for its corrosion resistance. Since the AISI304 has low thermal conductivity and high expansion it is challenging to weld it with AA6063 as both have different melting temperatures.



a)



b)

Fig. 2. a) Pressure measuring device, b) experimental set-up

2.2. Experiments

To secure the parent material and gauge the axial force exerted during friction welding, a dedicated pressure measuring apparatus (depicted in figure 2a) with suitable fixtures is constructed. This device incorporates a bottle-type hydraulic jack with a capacity of two tons, a drill chuck capable of holding workpieces up to a diameter of 20 mm, and a pressure gauge capable of measuring pressures up to 210kg/cm². Figure 2b illustrates the experimental setup comprising the specialized fixture affixed to the lathe machine. The

fixture, housing a tapered rod, is inserted into the tailstock of the lathe. One of the parent materials is held in the spindle (within the chuck), while the other material is secured in a drill chuck attached to the fixture. During the friction welding process, the axial force can be adjusted by manipulating the tailstock quill positioned within the lathe's tailstock. Vibrations generated during welding are mitigated using a jig installed between the chuck and the apron. This arrangement effectively reduces vibrations during welding, with pressure readings displayed on the pressure gauge.

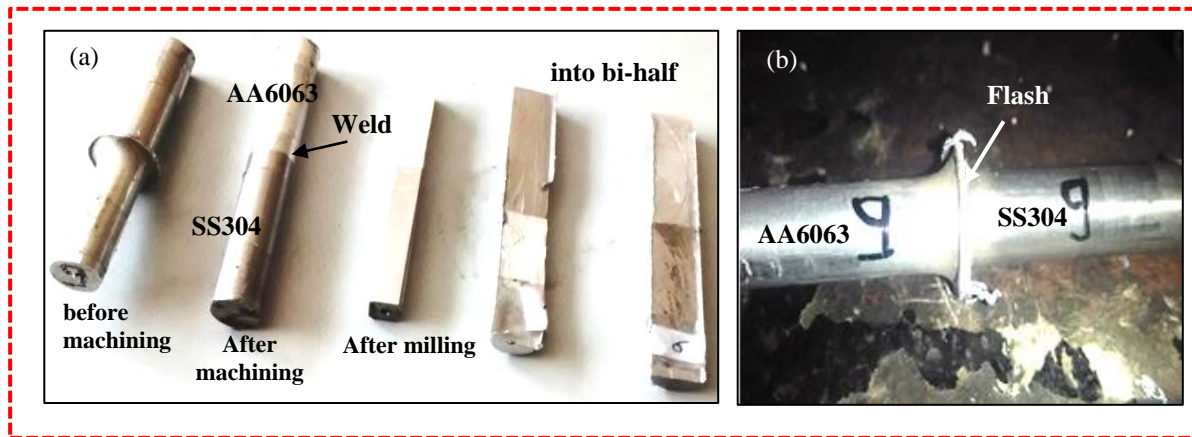


Fig. 3. a) Friction welded bimetallic joints, b) flash formation

Sample rods of steel and aluminium, each with a diameter of 12 mm, are cut into pieces measuring 45 mm in length. The pressure measuring device is secured in the tailstock using a tapered rod and base plate, while a jig is attached between the spindle and drill chuck. Pressure is applied via the handle in the tailstock, while friction time and forging time are measured using a stopwatch. Turning operations are conducted to remove the flash generated around the weld zone. Figure 3a depicts the samples before and after the welding and turning operation. Figure 3b portrays the bimetallic weld with flash generation. In this study, the choice of destructive tests was guided by the process objective. A range of testing methods can be utilized to assess the characteristics of the weld. Specifically, a Rockwell hardness testing machine was employed to measure hardness, while the prediction of impact strength was conducted using a Charpy testing machine.

2.3. Process Optimization

In addition to traditional welding methods, friction welding offers control over various welding parameters. These parameters encompass the diameter of the experimental rod, rotational speed of the parts,

duration of frictional contact, delay time before forging, friction pressure, part geometry, material properties, and more. One of the key objectives of this study is to optimize input parameters such as rpm, friction time, and friction pressure during the welding process. The applied pressure during welding holds significant importance as it governs the temperature gradient and rotational torque. Friction pressure must be sufficiently high to facilitate the removal of oxides and ensure uniform heating throughout the process. The implementation of friction welding enhances welding properties. Friction time should be calibrated to allow for plastic deformation or the removal of any potential residues and particles. Taguchi-L9 array technique was used in this study to optimize the friction welding parameters. The Taguchi method offers a systematic framework for identifying the optimal combination of inputs to achieve desired product outcomes. It introduces a novel approach to experiment design, guided by clear principles. Central to this method is an orthogonal array, a specialized set of arrays that dictate how experiments are conducted with the minimum number necessary to comprehensively capture the factors influencing performance parameters. Figure 4 illustrates the typical Taguchi design method.

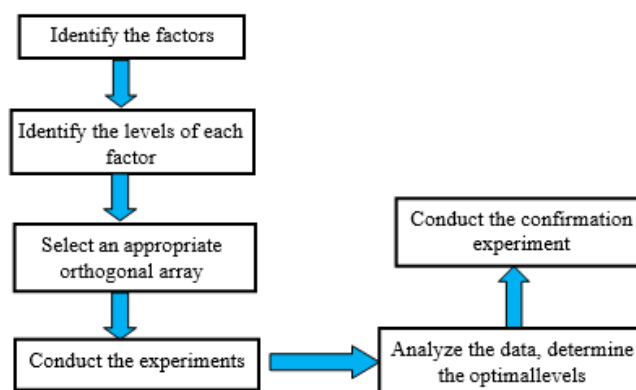


Fig. 4. Flow chart of Taguchi design of experiment

By understanding the quantity of parameters and levels involved, one can select the suitable orthogonal array. Utilizing the array selector table, the specific array name can be identified by locating the intersection of the respective columns and rows representing the parameter and level counts. Table 2 displays the parameters and their corresponding values across various levels during friction welding. Given our experiment entails three parameters, the L9 array is chosen. In the L9 array, as illustrated in table 3, parameter 1 denotes speed, parameter 2 denotes pressure, and parameter 3 denotes time. Level 1 is represented by 1, level 2 is represented by 2 and level

3 is represented by 3. This experimentation aims to know the interactions of various parameters.

Table 2. RFW Parameters and their levels

Welding Parameters [Unit]	Levels		
	1	2	3
Pressure [MPa]	8	10	12
Speed [rpm]	800	1000	1200
Time [s]	10	15	20

Table 3. Taguchi L9 array

Run/ Exp. No.	Welding parameters			Response Parameters	
	Pressure [MPa]	Speed [rpm]	Time [s]	Hardness [HRC]	Energy [J]
1	8	800	10	40	32
2	8	1000	15	60	28
3	8	1200	20	70	22
4	10	800	15	45	30
5	10	1000	20	63	27
6	10	1200	10	83	20
7	12	800	20	50	29
8	12	1000	10	65	26
9	12	1200	15	85	18

3. RESULTS AND DISCUSSION

Initially, cylindrical cross-sectional samples were prepared for friction welding and the dissimilar friction welds were prepared. The optical microstructure was taken near the weld zone and shown here in figure 5a. No defects, infusion or cracks were found. It shows the strong bond between two dissimilar samples and the narrow weld zone was seen. Subsequently, a hardness test was conducted in the vicinity of the weld zone following the cutting of specimens along their length. Two parallel lines were drawn at diametrically opposite ends of the workpiece, and two points were marked on the aluminium side and two on the stainless-steel side from the weld zone, total five marked points including the weld zone itself. Readings were then recorded accordingly. For the Izod impact test, U-notch specimens were prepared from the welded specimen sized at 75 mm x 10 mm x 10 mm. The machine needle was adjusted to 0°, and upon releasing the hammer, the welded specimen underwent failure due to the intense impact. The results obtained from the experimental work are presented in figures 5b and 5c. Visual representations of the hardness test and impact test specimens are provided in figure 6. The hardness test was conducted in the vicinity of the weld zone by applying load with a dwell time of 10 s. According to the results, speed and time determine the hardness. The increase in speed may lead to generating high heat in the vicinity of joints. This leads to an increase in

temperature and sudden cooling in the presence of air. This is a type of air-quenching process, moreover; the aluminium shows age hardening.

The combination of an increase in speed and time will lead to an increase in the hardness of the samples. Taguchi analysis aims to optimize processes by identifying the most efficient solution to a given problem. This method is often implemented using software like Minitab 7, which is specifically designed to support Taguchi experimentation. Minitab serves as an analytical tool, enabling users to effectively apply Taguchi methods in their optimization endeavours. From tables 4, 5, 6 and 7; parameters pressure, speed, and time represent the response of each property. The larger the better configuration is chosen for Taguchi analysis. Taguchi analysis of Hardness: mean hardness versus pressure, speed, and time.

Table 4. Response table for means (Hardness)

Level	Pressure	Speed	Time
1	56.67	45.00	62.67
2	63.67	62.67	63.33
3	66.67	79.33	61.00
Delta	10.00	34.33	2.33
Rank	2	1	3

Table 5. Response table for means (impact energy)

Level	Pressure	Speed	Time
1	27.33	30.33	26.00
2	25.67	27.00	25.33
3	24.33	20.00	26.00
Delta	3.00	10.33	0.67
Rank	2	1	3

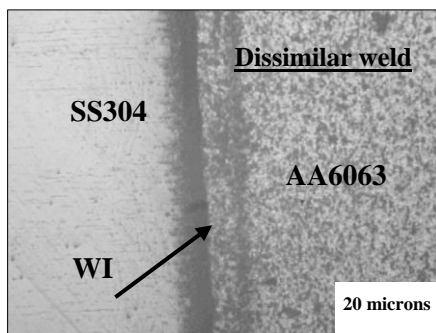
Table 6. Response for signal-to-noise ratio (hardness)

Level	Pressure	Speed	Time
1	34.84	33.03	35.56

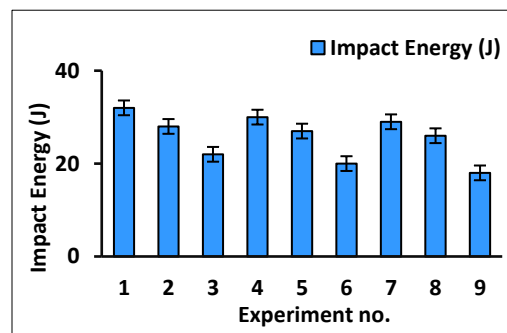
2	35.81	35.94	35.74
3	36.28	37.96	35.62
Delta	1.44	4.93	0.18
Rank	2	1	3

Table 7. Response for signal-to-noise ratio (impact energy)

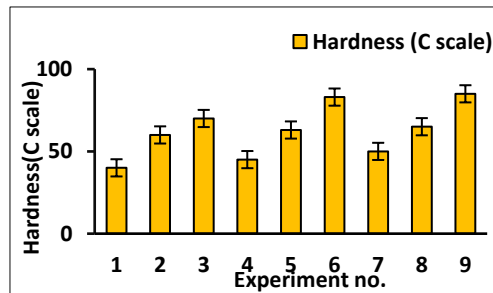
Level	Pressure	Speed	Time
1	28.63	29.63	28.14
2	28.06	28.62	27.86
3	27.55	25.99	28.24
Delta	1.08	3.64	0.38
Rank	2	1	3



a)

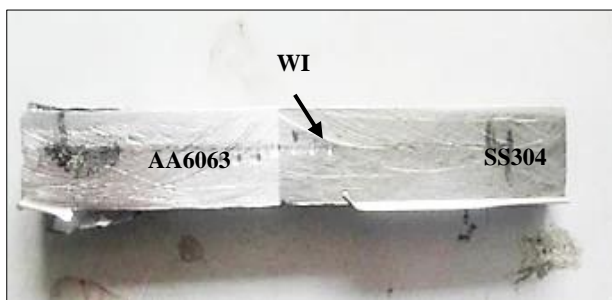


b)



c)

Fig. 5. a) Microstructure of AA6063-SS304 dissimilar friction weld; b) impact energy; c) average hardness



a)



b)

Fig. 6. Samples: a) FW sample after hardness test, b) FW sample after impact test

The main effects plot and signal-to-noise ratios plots in figures 7, 8, 9 and 10 respectively, generated using Minitab software, illustrate the mean values for

the hardness of the weld zone. At 8 MPa pressure, the mean hardness is approximately 56.67, while at 10 MPa it rises to around 66.67. Similarly, at 800 rpm

speed, the value of mean hardness was 45.00 which rises to 79.33 at the speed of 1200 rpm. The mean values obtained for time are also presented in table 4. Upon calculating delta values, it was evident that speed ranked highest in influencing weld zone hardness, while time exhibited the least impact, with a delta value of 2.33 in comparison to speed in rpm, which had a delta value of about 34.33. In figure 8, the main effects plot illustrates the mean impact energy values. At a speed of 800 rpm, the mean energy absorbed is approximately 30.33, while at 1200 rpm, it decreases to around 20.00. Similar mean values were observed for other parameters, such as pressure and time, as detailed in table 5. Upon analysing the delta values, it

is evident that speed ranks highest in influencing the impact energy of welded specimens, whereas time has the least effect. Taguchi Analysis of impact energy: mean energy absorbed versus pressure, speed, and time. Figures 9 and 10 display the response plot for the signal-to-noise ratio for hardness and impact energy, respectively, of the weld zone, generated using Minitab software. The mean values obtained are documented in tables 6 and 7. The table highlights that speed emerges as the primary parameter influencing the weld zone, while time has the least impact.

In the Taguchi analysis for signal-to-noise ratio, the mean of the S/N ratio is compared against parameters pressure, speed, and time.

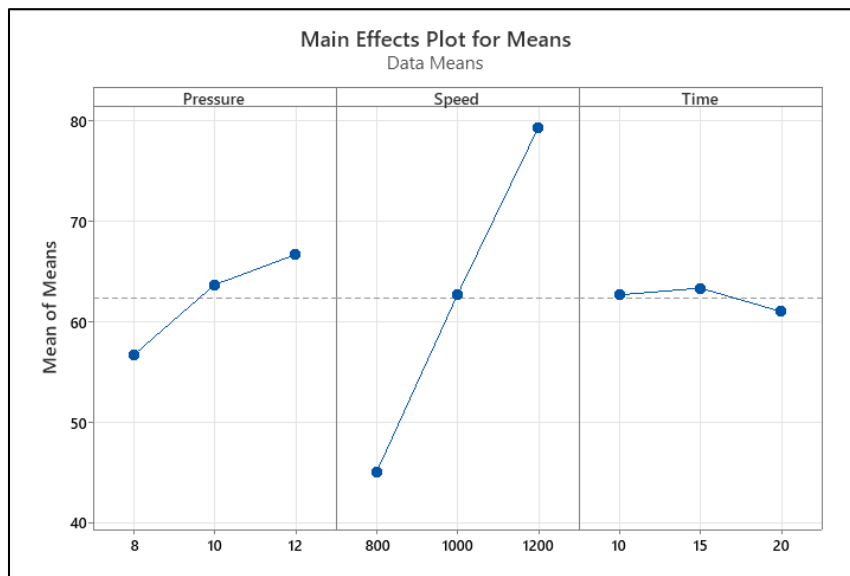


Fig. 7. Response for hardnesses means

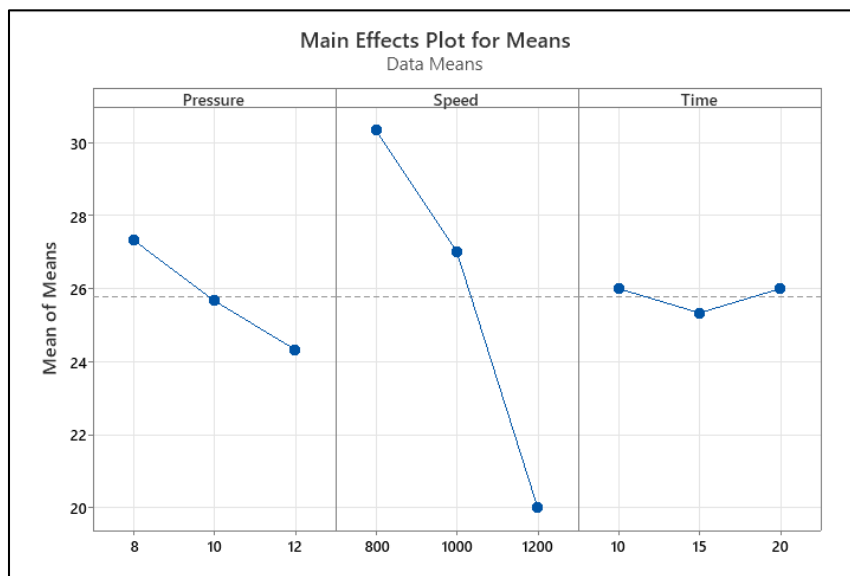


Fig. 8. Response for impact energy means

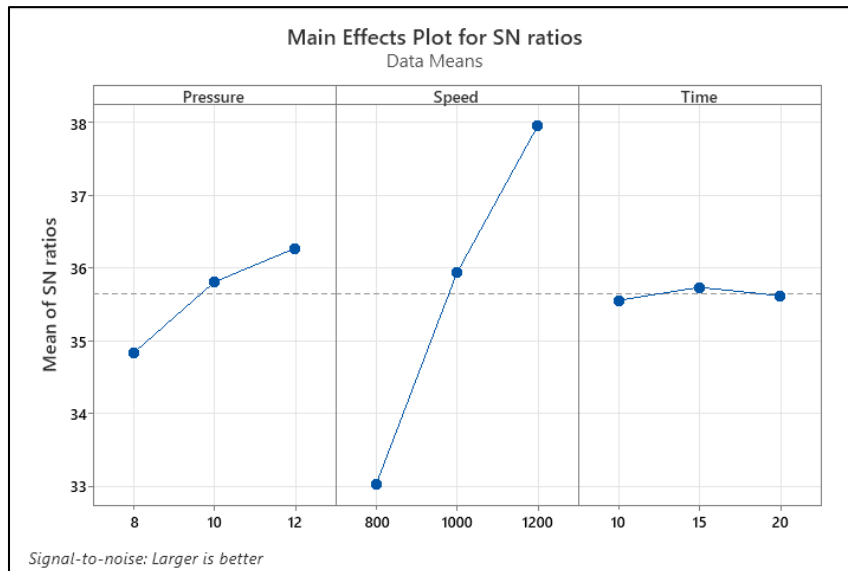


Fig. 9. Response for hardness signal-to-noise ratio

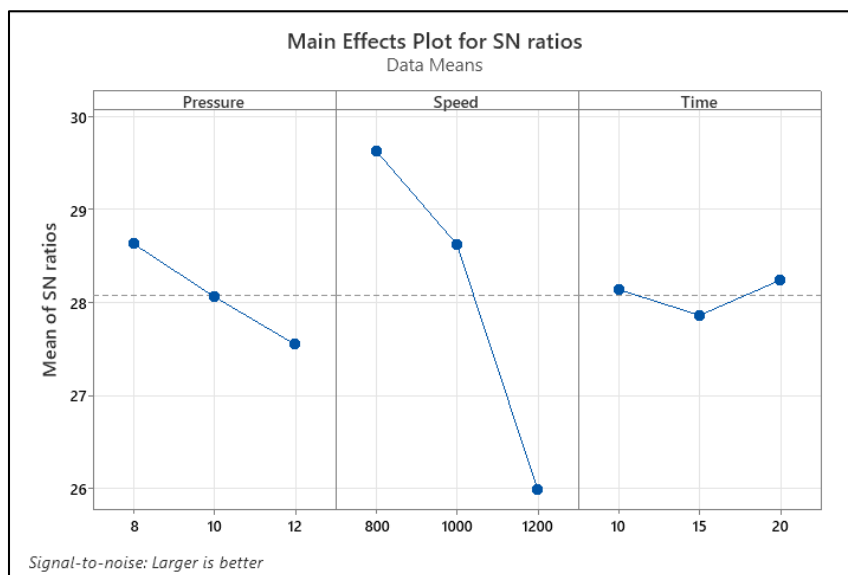


Fig. 10. Response for impact energy signal-to-noise ratio

3.1. Multi-Response Optimization

Taguchi-Grey relational analysis is a popular method used in manufacturing, electronics, and automotive industries to improve performance and efficiency. It evaluates multiple variables simultaneously to identify the optimal combination of parameters and streamline processes [13]. The analysis process starts with selecting control factors and their corresponding levels. These factors are chosen based on their potential impact on the response variables. An orthogonal array design, such as the L9 design, is then used to conduct a series of experiments with different combinations of factor levels. The response variables are measured, and the data is analysed to determine the extent to which each factor influences the responses [14]. The GRG (Goodness of

Resemblance Graph) indicates the degree of similarity between the ideal answer and the actual response obtained from the studies. A higher GRG value indicates that the factor has a greater impact on the response variable. GRG values help identify optimal parameter settings, which are confirmed through experiments. The Taguchi-Grey relational analysis method offers a comprehensive understanding of the factors that impact responses and an efficient way to identify optimal settings without many experimental runs [15-17].

3.1.1. Taguchi - Grey Relational Analysis for Parameters Optimizing

Signal-to-Noise(S/N) ratio calculation: The first step in Taguchi-based Grey Relational Analysis

(GRA) is to calculate the S/N ratio for the correlating responses [18]. There exist two potential outcomes that require deliberation:

i) The higher the better:

This scenario requires maximizing the Material Removal Rate (MRR), which aims for a higher S/N ratio in RUM.

$$S/N \text{ ratio } (y) = -10\text{Log}_{10}\left(\frac{1}{n} \sum_{i=1}^n \frac{1}{y_{ij}^2}\right) \quad (1)$$

ii) Lower-the-better:

The "lower-the-better" criterion is used to minimize the response variable, such as SR in this study. A lower S/N ratio indicates better performance.

$$y = -10\text{Log}_{10}\left(\frac{1}{n} \sum_{i=1}^n \frac{1}{y_{ij}^2}\right) \quad (2)$$

3.1.2. S/N ratio Normalization

After calculating the S/N ratio for the relevant replies, the next step is to standardize or normalize it. This is important because the units and ranges of various response variables can be different. Linear normalization is a method that is used to standardize a sequence so that it can be compared. The grey relational generation [19] refers to the process of normalizing the S/N ratio in the context of GRA.

The following formulae [16] transform Y_{ij} into the comparability sequence X_{ij} .

(i) For larger the better approach

$$x_{ij} = \frac{\max(Y_{ij,i=1,2,\dots,n})}{\max(Y_{ij,i=1,2,\dots,n}) - (\min Y_{ij,i=1,2,\dots,n})} \quad (3)$$

(ii) For smaller the better approach

$$x_{ij} = \frac{(Y_{ij,i=1,2,\dots,n}) - Y_{ij}}{(Y_{ij,i=1,2,\dots,n}) - Y_{ij} - (\min Y_{ij,i=1,2,\dots,n})} \quad (4)$$

3.1.3. Grey Relational Coefficient (GRC)

To establish the relationship between the ideal (best=1) and practical experiment outcomes, the GRC is computed for normalized data Equation 5 expresses the grey relational coefficient:

$$\delta(x_o(k), x_i(k)) = \frac{\Delta \min + \xi \Delta \max}{\Delta o_j(k) + \xi \Delta \max} \quad (5)$$

where $j = 1, 2, \dots, n$; and $k = 1, 2, \dots, m$, where n is the number of investigational data objects and m is the total number of replies, the reference sequence is denoted by $x_o(k)$, whereas the comparison sequence is denoted by $X_u(k)$, $o_j = \|x_o(k) - x_j(k)\|$, where $x_o(k)$ and $x_j(k)$ are the absolute differences, The minimum and maximum values of $x_j(k)$, known as quality loss functions, are \min and \max , is coefficient, which ranges from 0 to 1, with [0,1] depending on the

individual requirements. The most common value is 0.5 [20].

3.1.4 Grey Relational Grade (GRG) Weight Generation

The GRG is determined by calculating the average of GRCs using Equation 6 [21].

$$(X_o, x_i) = \frac{1}{\rho} \sum_{i=1}^{\rho} \delta(x_o(k), x_i(k)) \quad (6)$$

where $\delta(x_o, X_u)$ denotes the grey relational grade of the i^{th} trial and denotes the total number of answers. Weights are assigned to individual Grey Relational Grades to account for their effect on overall process performance. The weighted grey relational grade (WGRG) is obtained using Equation 7. The levels with the highest WGRG are considered optimal.

$$y_{ew}(x_o, x_i) = \frac{1}{\rho} \sum_{i=1}^{\rho} \delta(x_o(k), x_i(k)) + w_2(\delta(x_o(k), x_i(k))) \quad (7)$$

3.1.5. Optimum parameters with their levels

To analyse the GRG (Grey Relational Grade) values for each run, we generate a weighted grey relational grade. The higher-the-better technique is used to assess the GRG, where a larger value refers to better performance. The GRG values are then used to determine the optimal parameters and their respective levels. We calculate the average GRA (Grey Relational Analysis) for each input factor at each level and then choose the level with the highest GRG as the best option.

3.2. Relational Analysis

S/N ratio data for MRR and SR from nine runs is represented in table 8 and were normalized using equations 3 and 4, respectively, and the outcomes are presented in table 9. To normalize the data for S/N ratios, the min-max normalization is used, which scales the values to a range between 0 and 1. Firstly identify the minimum and maximum values in the data set for each factor. The normalized values have been calculated as shown in table 9. This shows the relation between the hardness and the energy absorbed.

The Grey Relational Coefficients (GRCs) were determined by normalizing the Signal-to-Noise (S/N) ratios. Equation 5 was used, with all input variables assigned the same importance value of 0.5. Next, using equation 7, the Weighted Grey Relational Grade was computed for both output responses, with a weightage of 0.5.

Table 10 shows the GRCs and GRGs values obtained for all nine runs.

Table 8. S/N ratio data of response parameters

Exp. No	S/N Ratio Values	
	Hardness	Impact energy
1	32.04119983	30.10299957
2	35.56302501	28.94316063
3	36.9019608	26.84845362
4	33.06425028	29.54242509
5	35.98681099	28.62727528
6	38.38156185	26.02059991
7	33.97940009	29.24795996
8	36.25826713	28.29946696
9	38.58837851	25.1054501

Table 9. Normalized data of S/N Ratios

Exp. No	Normalized values of S/N ratio	
	Hardness	Impact energy
1	1	0
2	0.462085068	0.232081533
3	0.257579302	0.651228362
4	0.843741786	0.11216987
5	0.397357037	0.29528958
6	0.03158867	0.816880289
7	0.70396405	0.171091775
8	0.355895492	0.360883393
9	0	1

Table 10. Computed GRGs along with GRGs

Exp. No.	Grey Relation Coefficient		Grade	Rank
1	1	0.333333333	0.333333	1
2	0.481735048	0.394347123	0.219021	7
3	0.402440172	0.589086602	0.247882	6
4	0.761895226	0.36027464	0.280542	3
5	0.453455939	0.415037499	0.217123	9
6	0.340504047	0.731936134	0.26811	4
7	0.628112336	0.376248706	0.25109	5
8	0.437023014	0.438936626	0.21899	8
9	0.333333333	1	0.333333	1

Table 10 displays GRG values that range randomly from 0 to 1. These values represent the connection between the reference and comparability sequences. A larger GRG score indicates stronger multi-performance attributes, meaning that higher GRG scores demonstrate better overall performance regardless of specific performance parameters. According to table 10, the input parameter values for run orders 1 and 9 result in the highest GRG based on

the experimental design assessment. Therefore, both experiments are the best option for selecting parameters that can maximize hardness and energy absorbed, displaying the highest level of multi-performance attributes.

After calculating the GRG values, the Taguchi approach can be utilized to tune GRG, simplifying the issue of multi-performance characteristics to a single GRG optimization.

Table 11. Response for means of grades

Factor	Levels			Delta	Rank
	1	2	3		
Pressure	0.2667	0.2553	0.2678	0.0125	3
Speed	0.2883	0.2184	0.2831	0.0699	1
Time	0.2375	0.2776	0.2387	0.0389	2

The results obtained for the grade are shown in table 11, indicating that spindle speed has the greatest influence on friction welding. Mean effects and signal-to-noise ratio plots for grade are depicted in figures 11 and 12, respectively. A response plot for a signal-to-noise (S/N) ratio where "larger is better" is used to identify the optimal settings of various factors that maximize the desired response while minimizing variability as shown in figure 12. The slope of the lines indicates the main effect of each factor. Steeper slopes suggest that the factor significantly impacts the response. The highest point on the plot for each factor level suggests the optimal setting for that factor to

maximize the S/N ratio. If the plot includes multiple lines for different conditions or interactions, the interaction effects can be observed by comparing the relative positions and slopes of these lines. The figure shows that the optimum values of pressure, speed and time are 12 MPa, 800 RPM and 15sec. respectively. To achieve the optimal condition where maximum hardness and energy are absorbed, the highest values of the grade obtained need to be observed. In this case, scatter plots indicate that pressure at level 3, speed at level 1, and time at level 2 are the ideal values to attain the desired welding conditions.

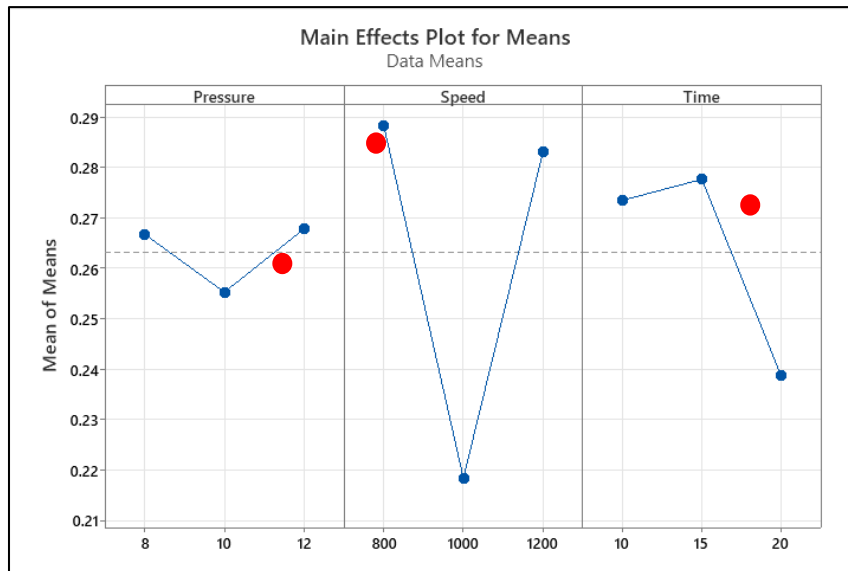


Fig. 11. Response for grade means

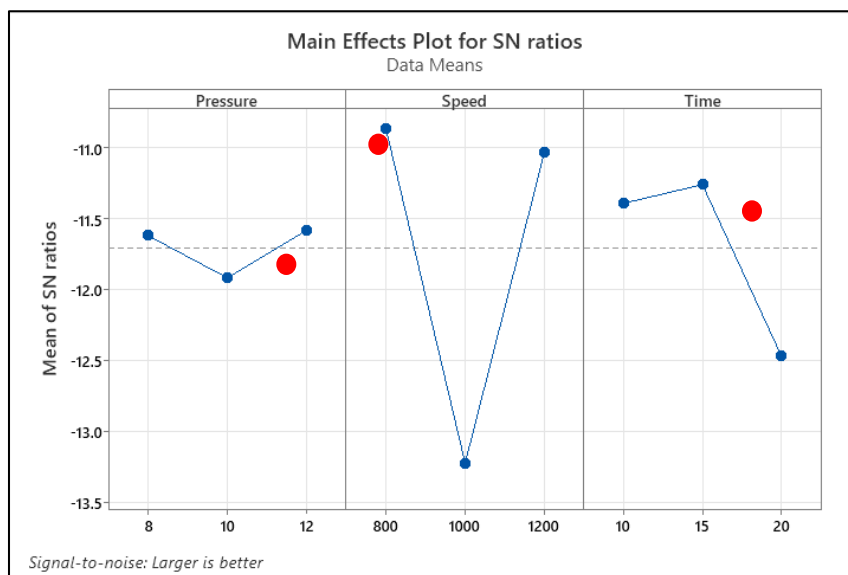


Fig. 12. Response for grade signal-to-noise ratio

4. CONCLUSIONS

RFW has proven as a successful method in joining SS304 and AA6063 materials for industrial applications. The versatility of this process extends to various weldable materials, including those typically not joined by conventional welding methods. The hardness and impact energy tests confirmed that the joints had satisfactory strength. Hardness was obtained in the range of 40-85HR_C and Impact strength was in the range of 18-32 J for the developed dissimilar joints. The analysis of response tables and plots generated using Minitab software has provided some valuable insights.

The welding speed parameter was the most influential parameter. The grey relational analysis has provided the optimal conditions that can yield the best

weld during the welding process. The optimum values are 12 MPa friction pressure, 800 RPM speed and 15 sec weld time. The combination of increase in speed and time will lead to the increase in the hardness of the samples.

REFERENCES

- [1] Taban E., Gould J. E., Lippold J. C., *Dissimilar Friction Welding of 6061 Aluminium and AISI 1081 Steel, Properties and Microstructural Characterization*, Materials & Design, vol. 31, 2010, pp. 2305-2311.
- [2] Khalid Rafi H., Janaki Ram G. D., Phanikumar G., Prasad Rao K., *Microstructure and Tensile Properties of Friction Welded Aluminum Alloy AA7075-T6*, Materials & Design, vol. 31, iss. 5., 2010, pp. 2375-2380.
- [3] Uzkut M. et al., *Friction Welding and its Applications in Today's World*, Proceedings of the 2nd International Symposium on Sustainable Development, 2010, pp. 8-9.

- [4] **Sandeep Kumar et.al.**, *To Study the Mechanical Behavior of Friction Welding of Aluminium Alloy and Mild Steel*, International Journal of Mechanical Engineering, and Robotic Research, ISSN 2278 – 0149, Vol. 1, No. 3, 2012, pp. 43-50.
- [5] **Shubhavardhan R. N. Surendran S.**, *Friction Welding to Join Stainless Steel and Aluminum Materials*, International Journal of Metallurgical & Materials Science and Engineering, ISSN 2278- 2516, Vol.2, Issue 3, 2012, pp. 53-73.
- [6] **Hascalik A., Orhan N.**, *Effect of particle size on the friction welding of Al₂O₃ reinforced 6160 Al alloy composite and SAE 1020 steel*, Materials & Design, vol. 28, iss. 1, 2007, pp. 313–317.
- [7] **Alveset E. P., Neto F. P., An Ch. Y.**, *Welding of AA1050 Aluminum with AISI 304 Stainless Steel by Rotary Friction Welding Process*, Journal of Aerospace Technology and Management, vol. 2, no. 3, 2010, pp. 301-306.
- [8] **Ofem U. U., Colegrove P. A., Addison A., Russell M. J.**, *Energy and Force Analysis of Linear Friction Welds in a Medium Carbon Steel*, Science and Technology of Welding & Joining, vol. 15, no. 6, 2010, pp. 479-485.
- [9] **Sahin M., Akata H. E., Ozel K.**, (2008), *An Experimental Study on Joining of Severe Plastic Deformed Aluminum Materials with Friction Welding Method*, Materials & Design, vol. 29, 2008, pp. 265–274.
- [10] **Senthil M. S., Noorul H. A., Sathiya, P.**, *Eco-friendly Frictional Joining of AA6063 and AISI304L Dissimilar Metals and Characterisation of Bimetal Joints*, Journal of New Materials for Electrochemical Systems, vol. 23, no. 2, 2020, pp. 101-111.
- [11] **Ruma, Wahed M. A., Farhan M.**, *A Study on the Effect of External Heating of the Friction Welded Joint*, International Journal of Emerging Technology and Advanced Engineering, vol. 3, iss. 5, 2013, pp. 603 - 613.
- [12] **Selvaraj R., Shanmugam K., Selvaraj P., Prasanna Nagasai B., Balasubramanian V.**, *Optimization of Process Parameters of Rotary Friction Welding of Low Alloy Steel Tubes using Response Surface Methodology*, Forces in Mechanics, vol. 10, 2023, 100175, ISSN 2666-3597.
- [13] **Linnik S. A., Gaydaychuk A. V., Baryshnikov E. Y.**, *Deposition of Polycrystalline Diamond Films with a Controlled Grain Size by Periodic Secondary Nucleation*, Materials Today: Proceedings, 2016, vol. 3, S138-S144.
- [14] **Jain N., Kumar R.**, *Multi-response optimization of process parameters in friction stir welded aluminum 6061-T6 alloy using Taguchi grey relational analysis*, World Journal of Engineering, 2022, vol. 19, no. 5, pp. 707-716.
- [15] **Atapour S. M., Pourbabaee H., Asghari, M. A.**, *Multi-response optimization of surface roughness in turning of AISI 1045 steel using Taguchi-Grey relational analysis*, Materials Today: Proceedings, 2019, vol. 16, pp. 1374-1380.
- [16] **Lin C. C., Chen, C. L.**, *Optimization of surface roughness in finish turning of AISI 1045 steel using Taguchi-grey relational analysis*, Journal of Manufacturing Processes, 2019, vol. 38, pp. 1-10.
- [17] **Sahoo S. K., Dash P. K., Jena B. K.**, *Optimization of multi-response surface roughness characteristics in turning of AISI 1040 steel using Taguchi-grey relational analysis*. Materials Today: Proceedings, 2019, vol. 16, pp. 1745-1752.
- [18] **Haq A. N., Marimuthu P., Jeyapaul R.**, *Multi response optimization of machining parameters of drilling Al/SiC metal matrix composite using Grey relational analysis in the Taguchi method*, International Journal of Advanced Manufacturing Technology, 2008, vol. 37, pp. 250-255.
- [19] **Pawade R. S., Joshi S. S.**, *Multi-objective optimization of surface roughness and cutting forces in high-speed turning of Inconel 718 using Taguchi Grey relational analysis (TGRA)*, International Journal of Advanced Manufacturing Technology, 2011, vol. 56, pp. 47–62.
- [20] **Tosun N** (2006) *Determination of optimum parameters for multi-performance characteristics in drilling by using Grey relational analysis*. International Journal of Advanced Manufacturing Technology, 2016, vol. 28, pp. 450-455.
- [21] **Lin J. L., Lin C. L.**, *The use of the orthogonal array with Grey relational analysis to optimize the electrical discharge machining process with multiple performance characteristics*, The International Journal of Machine Tools and Manufacture, 2002, vol. 42, pp. 237–244.